Supplementary Information (SI) for Dalton Transactions.

Tailoring porphyrinic MOF-545 performances for CO_2 photocatalytic reduction through linker chlorination

Amanda Lyn Robinson, Sadiya Sadiya, Sandeep Kumar, Francesc Penas-Hidalgo, Khadija Talbi, Zakaria Halime, Mathieu Frégnaux, Damien Aureau, Maria Gomez-Mingot, Pierre Mialane, Albert Solé-Daura, Caroline Mellot-Draznieks, Anne Dolbecq

Electronic Supplementary Information

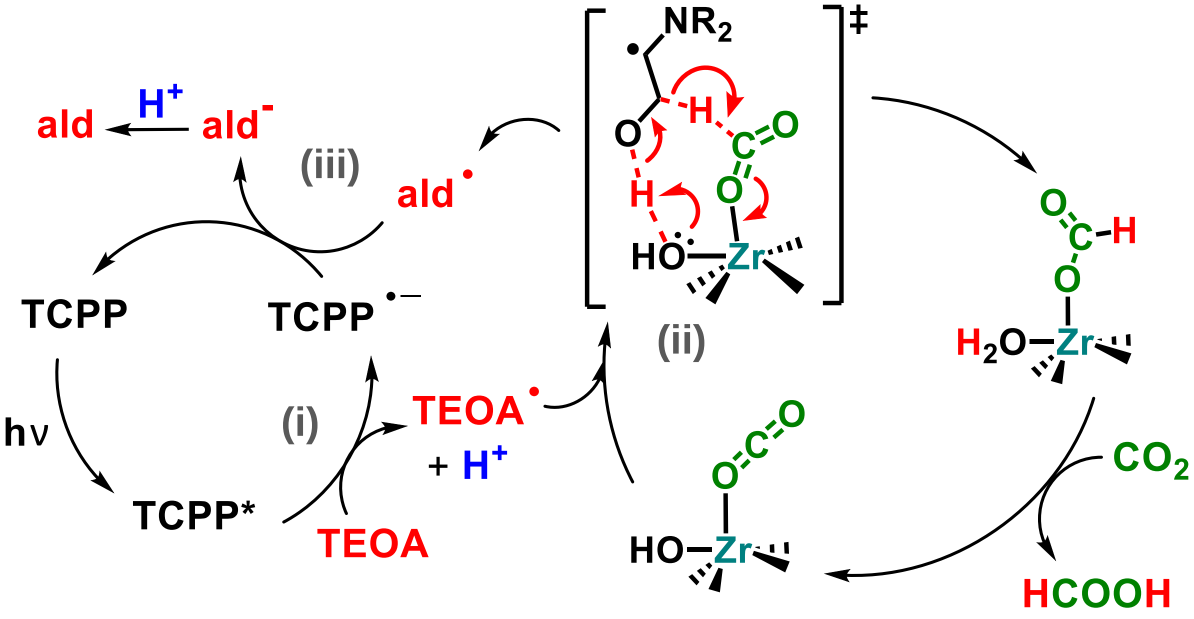

(i) Photo-oxidation of TEOA at the TCPP linkers
(ii) Thermally-activated hydrogenation of CO_2 at the Zr^{IV}_6 nodes
(iii) Termination

Fig. S1. Schematic summary of the proposed reaction mechanism promoted by Zr-based porphyrinic MOFs for the photocatalytic reduction of CO_2 to formic acid in presence of TEOA as sacrificial electron donor (R = CH_2CH_2OH). From Y. Benseghir, A. Solé-Daura, D. R. Cairnie, A. L. Robinson, M. Duguet, P. Mialane, P. Gairola, M. Gomez-Mingot, M. Fontecave, D. Iovan, B. Bonnett, A. J. Morris, A. Dolbecq and C. Mellot-Draznieks, *J. Mater. Chem. A*, 2022, **10**, 18103–18115

Table S1. Particle sizes determined by measuring the lengths of the particles shown in Figure 2.

Material	Particle Size Range (nm)	Mean Particle Size (nm)	Median Particle Size (nm)
MOF-545	680 – 2280	1226	1114
MOF-545 25% Cl	517 – 2422	1442	1368
MOF-545 50% Cl	464 – 1455	936	841
MOF-545 100% Cl	103 – 218	147	152

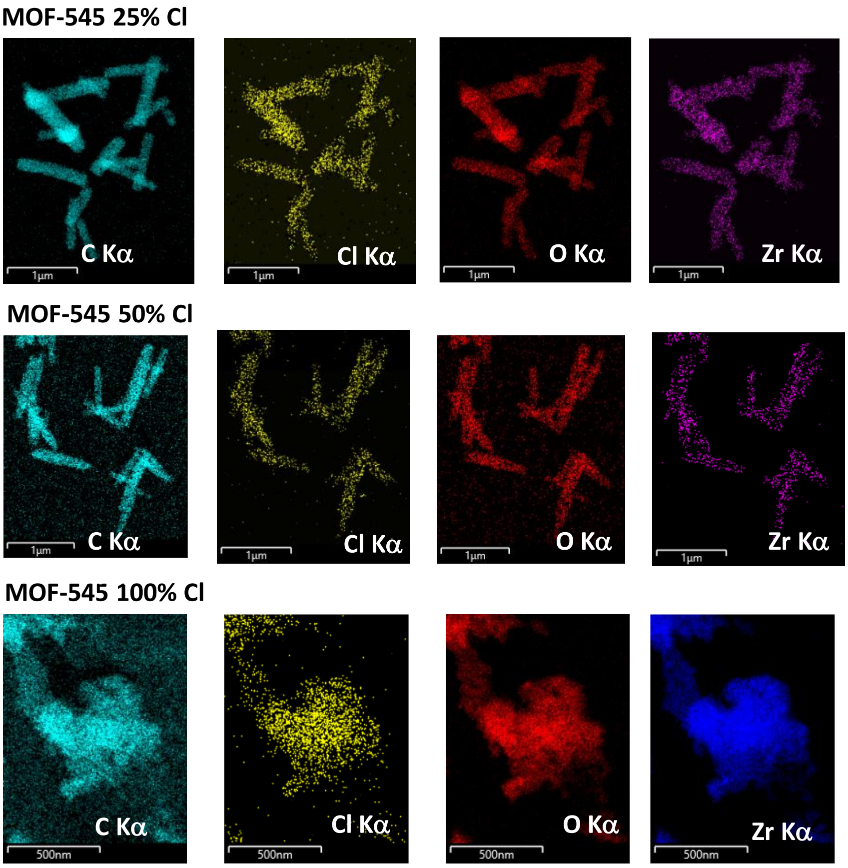

Fig. S2. STEM-EDS mapping of the composites.

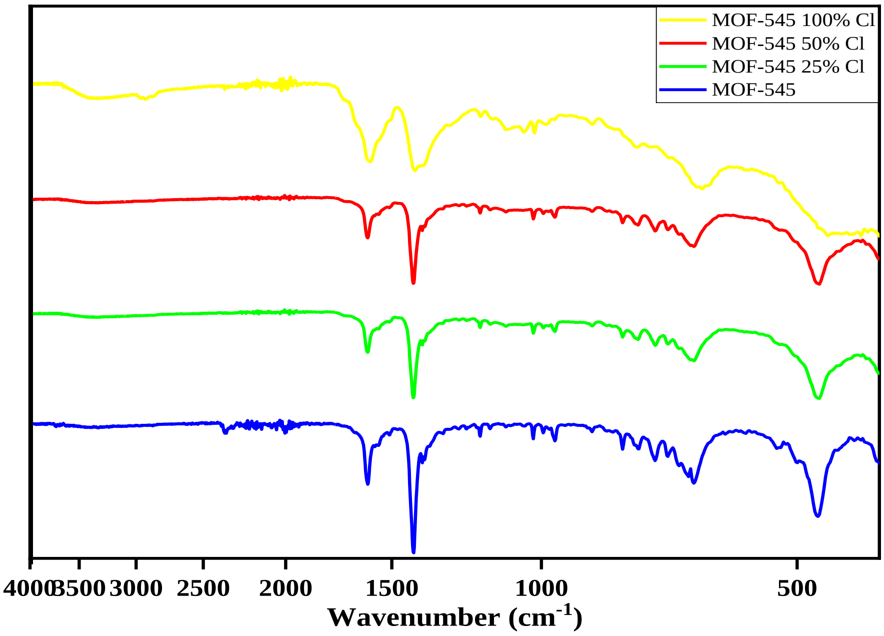

Fig. S3. IR spectra of MOF-545 (blue line), MOF-545 25% Cl (green line), MOF-545 50% Cl (red line) and MOF-545 100% Cl (yellow line)

Table S2. Experimental Cl/Zr ratio determined by SEM-EDX.

Material	**Experimental Cl/Zr atomic ratio given by EDX**
MOF-545	0.07
MOF-545 25% Cl	0.32
MOF-545 50% Cl	0.46
MOF-545 100% Cl	0.75

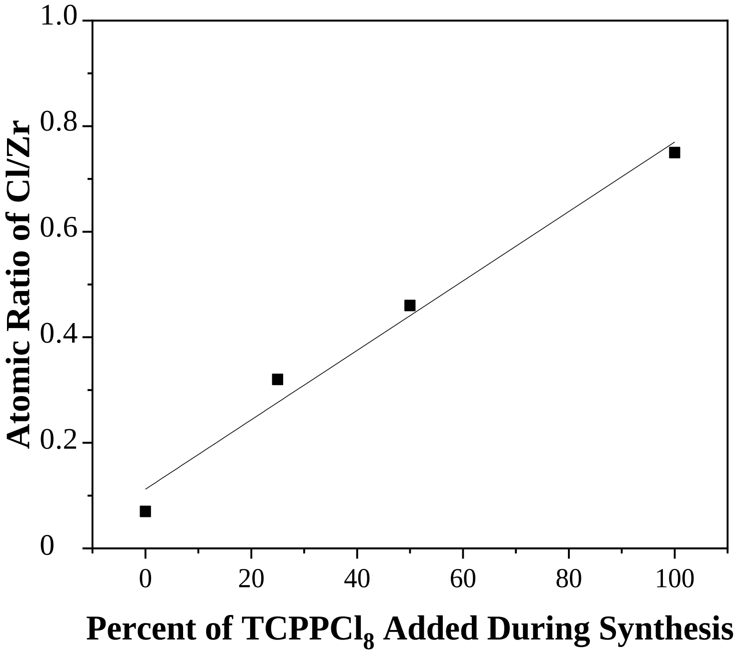

Fig. S4. Variation of the Zr/Cl atomic ratio determined by SEM EDX with the percentage of TCPPCl$_8$ linkers incorporated during the synthesis.

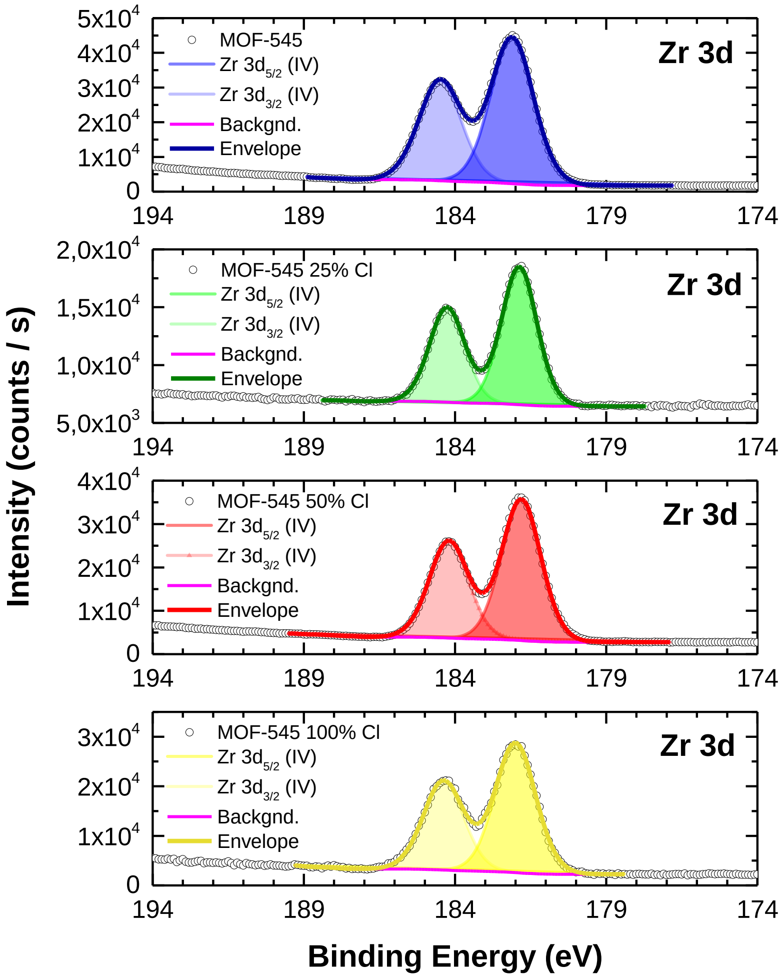

Fig. S5. X-Ray Photoelectron spectra on Zr3d region recorded for MOF-545 (blue line), MOF-545 25% Cl (green line), MOF-545 50% Cl (red line) and MOF-545 100% Cl (yellow line).

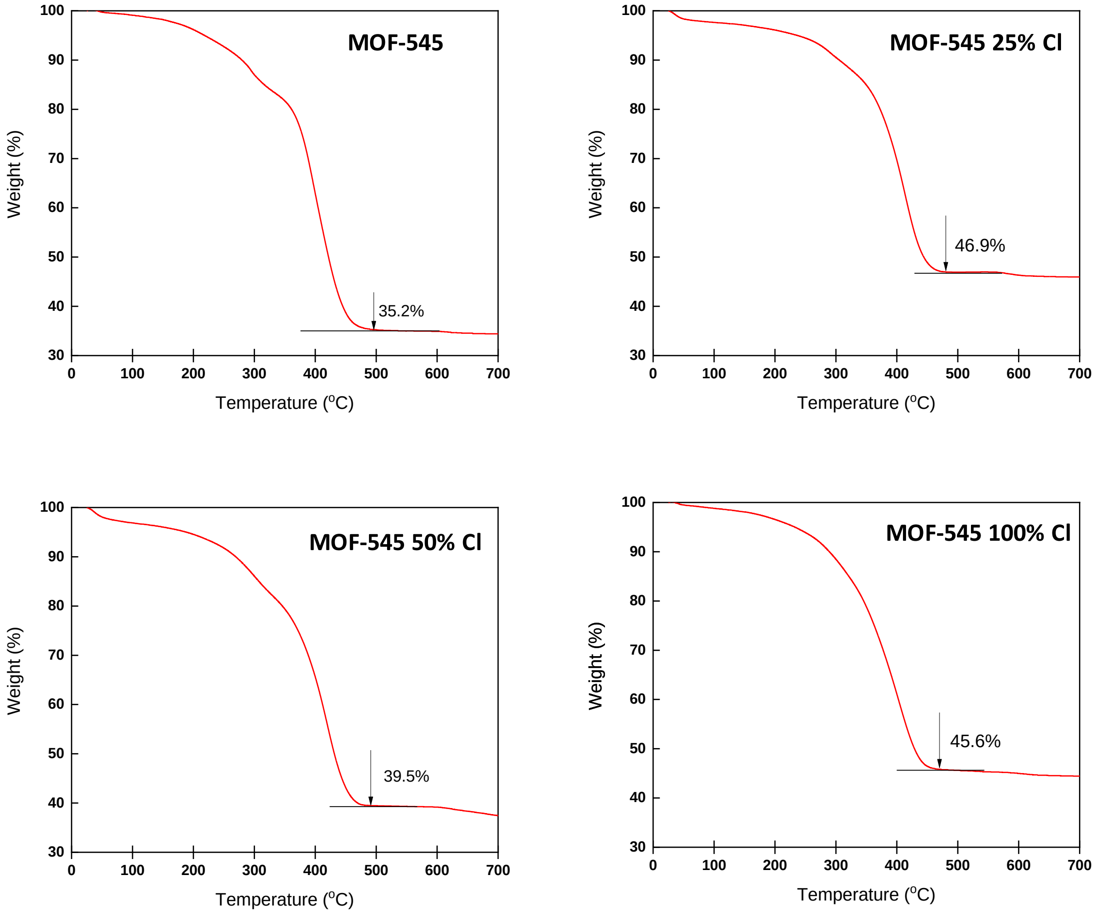

Fig. S6. TGA curves of the four MOF-545 derivatives in air.

Table S3. Proposed chemical formula and calculated and experimental mass losses.

Material	**Proposed Chemical Formula**	**M (g mol^{-1})**	**Residual mass**	
			Calc.	**Exp.**
MOF-545 25% Cl	$[Zr_6O_{16}H_{16.3}][TCPP]_{1.3}[TCPPCl_8]_{0.4}Cl_{1.5}\cdot H_2O$	2392	44.7	46.9
MOF-545 50% Cl	$[Zr_6O_{16}H_{17.5}][TCPP]_{1.0}[TCPPCl_8]_{1.0}Cl_{1.5}\cdot 4H_2O$	2723	39.2	39.5
MOF-545 100% Cl	$[Zr_6O_{16}H_{15.1}][TCPPCl_8]_{1.4}Cl_{1.5}$	2359	45.3	45.6

The formulas were derived from the experimental mass losses observed in the TGA curves and were also based on the following formula previously proposed for MOF-545: $[Zr_6O_{16}H_{17.5}][C_{48}H_{26}N_4O_8]_2Cl_{1.5}$.[1] Missing linkers were introduced for the two MOFs exhibiting the highest residual masses (MOF-545 25% Cl and MOF-545 100% Cl).

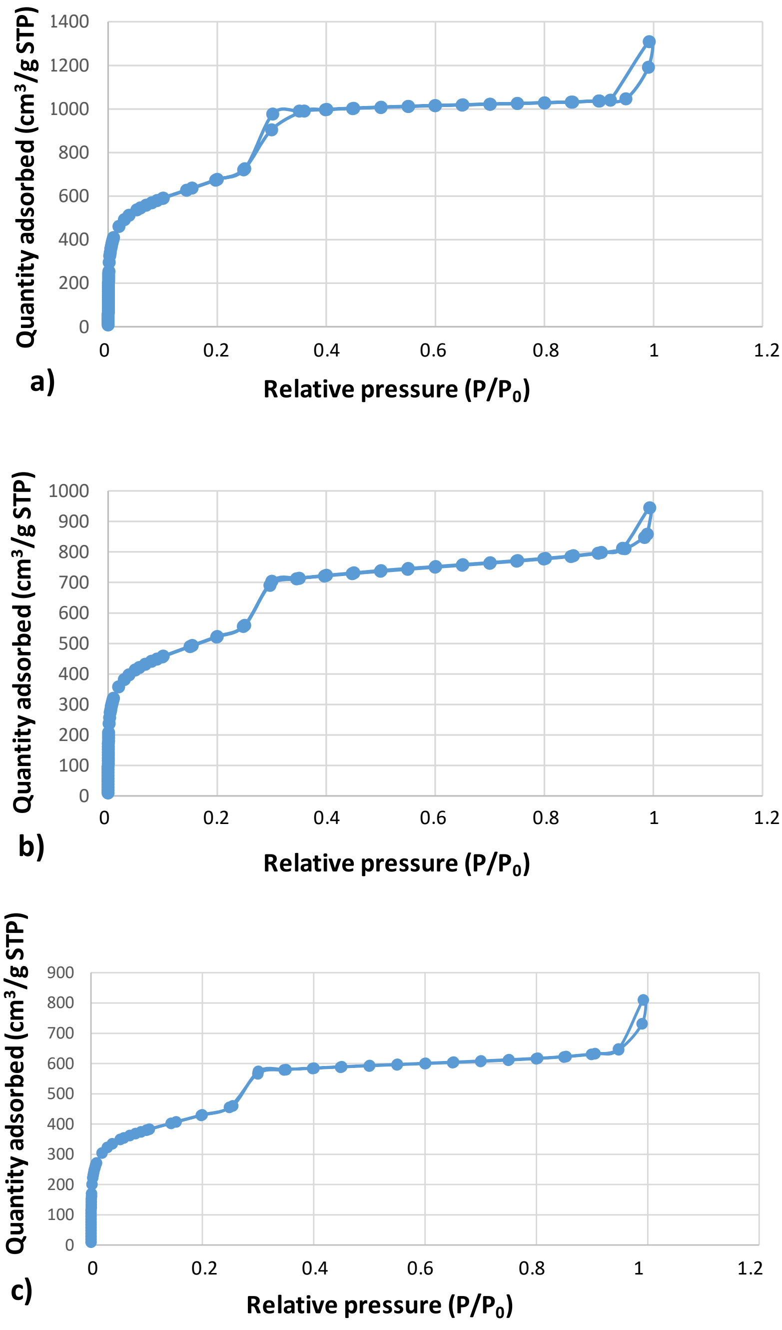

Fig. S7. N_2 adsorption isotherms at 77 K of a) MOF-545, b) MOF-545 25% Cl and c) MOF-545 50% Cl. BET surface area: 2412 m^2 g^{-1} (MOF-545), 1543 m^2 g^{-1} (MOF-545 25% Cl), 1867 m^2 g^{-1} (MOF-545 50% Cl).

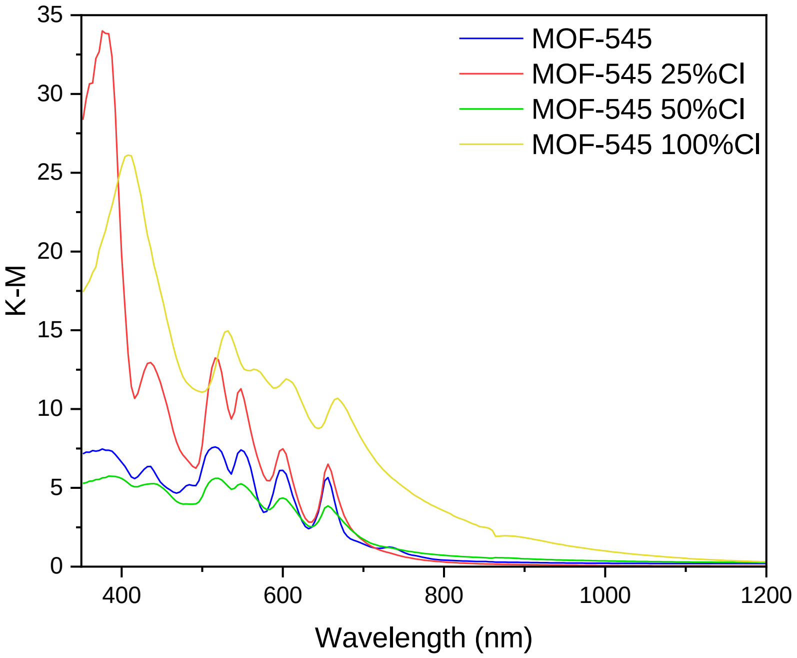

Fig. S8. Solid UV-vis spectra of the four MOFs.

Table S4. TON values (calculated with respect to Zr_6 clusters) and productions of the four MOFs, corresponding to Fig.6, calculated using the molar mass given in Table S3.

Catalyst	**Formate (µmol) after 16h**	**TON**	**Formate (µmol) after 2h**	**Rate production (µmol g^{-1} h^{-1})**
MOF-545	2.83	4	1.78	445
MOF-545 25 %	5.24	6	2.20	550
MOF-545 50%	7.39	10	2.50	625
MOF-545 100%	3.70	4	2.10	525

Table S5. Control experiments for the photocatalytic CO_2 reduction experiments using MOF-545.[a]

Entry	**Catalyst (mg)**	**CH_3CN (mL)**	**TEOA (mL)**	**Formate (µmol)**
1	2	1.9	0.1	1.78
2[b]	2	1.9	0.1	0.34
3[c]	2	1.9	0.1	0.34
4	-	1.9	0.1	0.28
5	2	2	-	0.35

[a] Reaction conditions: 2 mg of catalyst in 2 mL of CO_2-saturated solutions irradiated with a solar simulator with a 400 nm cut-off filter, reaction time 2 h. [b] Argon was used instead of CO_2.[c] No irradiation.

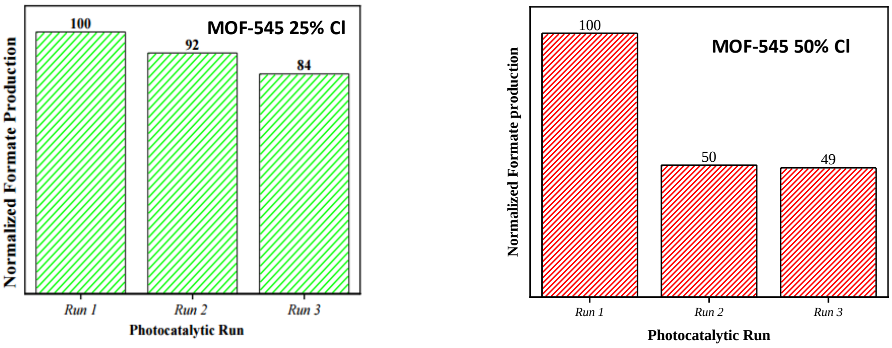

Fig. S9. Recyclability experiments for MOF-545 25% Cl (left) and MOF-545 50% Cl (right). Reactions conditions: 2 mg in 2 mL of CH_3CN/TEOA 20:1, 2 h irradiation.

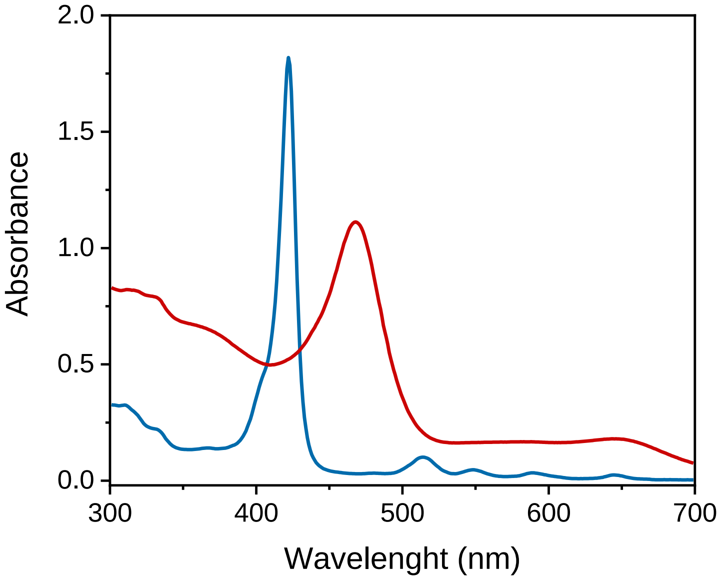

Fig. S10. UV-vis spectra of TCPP (blue) and $TCPPCl_8$ (red) in DMF.

Table S6. Compilation of key energetic parameters to compare the photooxidizing ability of TCPP and $TCPPCl_8$ linkers. Energies are given in kcal mol^{-1}.

Linker	ΔG reduction ($G_{red,doublet} - G_{ox,triplet}$)	λ_i (oxidized, triplet surface)	λ_i (reduced surface)	λ_i average
TCPP	-101.3	4.6	2.1	3.4
$TCPPCl_8$	-103.0	3.2	3.0	3.1

The qualitative analysis of the molecular orbital energies (Figure 7 of the main text) and the data compiled in Table S6, strongly suggest that the photo-oxidation of TEOA by the triplet excited state of the chlorinated linker is faster than that promoted by its non-chlorinated analogue. According to Marcus theory,[2] the free-energy barrier for a single-electron transfer depends on two key parameters: the thermodynamic driving force (ΔG_{SET}) and the reorganization energy (λ), which is the sum of the individual lambda values (λ_i) for both components, i.e. the donor and the acceptor. In the normal Marcus region (where $\lambda > -\Delta G_{SET}$), which is most common scenario, a larger driving force implies a lower barrier and therefore faster kinetics. In this system, we indeed expect to be in the normal region, given that the contribution of the TEOA/$TEOA^{+\cdot}$ pair to the reorganization energy is already quite large (>35 kcal mol^{-1}),[3] and therefore λ is expected to be greater than $-\Delta G_{SET}$. Since the contributions of the chlorinated and non-chlorinated porphyrins to the reorganization energy are small and comparable (3.4 and 3.1 kcal mol^{-1} for TCPP and $TCPPCl_8$, respectively), the height of the electron-transfer barrier is predominantly determined by the thermodynamic driving force. Because the reduction of $TCPPCl_8$* is more favorable than that of TCPP*, we therefore expect faster kinetics for quenching of the chlorinated linker.

Synthesis of TCPPCl$_8$

General Materials and Methods:

All solvents and other chemical reagents used in the synthetic route were obtained from commercial sources as guaranteed-grade reagents and used without further purification. 5,10,15,20-tetrakis(4-methoxycarbonylphenyl)porphyrin (TMPP) was purchased from PorphyChem company. Proton nuclear magnetic resonance (^{1}H NMR) spectra were recorded at room temperature on Bruker Advance 300 MHz spectrometers. The electrospray ionization high resolution mass spectrometry (ESI-HRMS) experiments were performed on TSQ (Thermo Scientific. 2009) with an ESI$^+$ method. Ground state absorption spectra were measured on a Specord double beam spectrophotometer (Analytik Jena).

Synthetic procedures for the synthesis of TCPPCl$_8$:

Porphyrin TCPPCl$_8$ was prepared by adapting previously reported procedures[4-6] as follows:

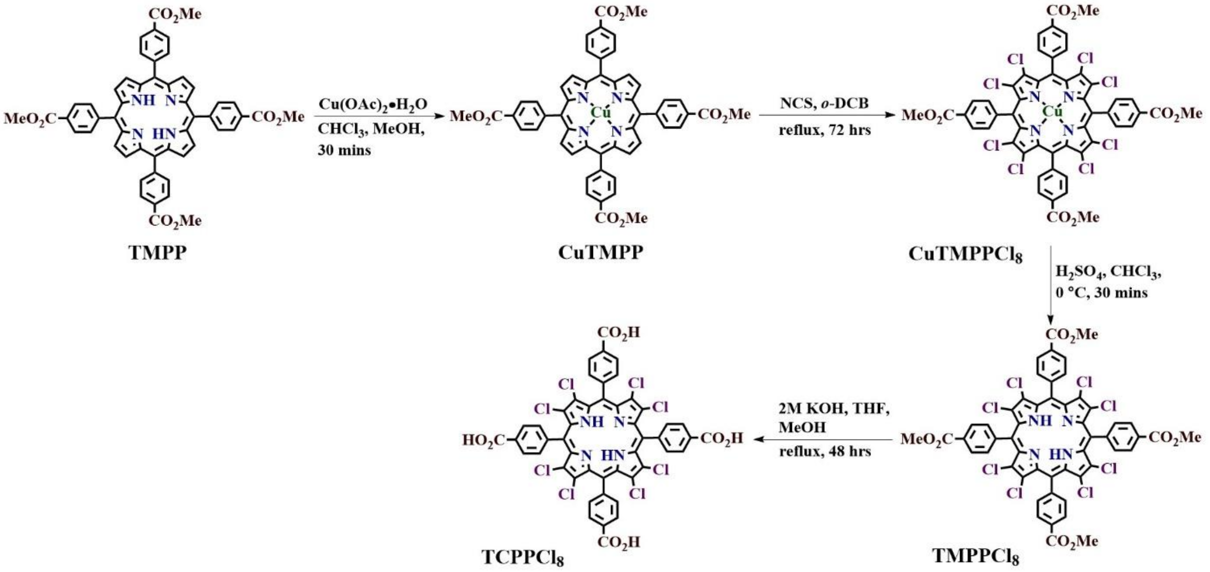

Fig. S11: Synthetic scheme for the synthesis of TCPPCl$_8$

Synthesis of Copper(II) 5,10,15,20-tetrakis(4-methoxycarbonylphenyl)porphyrin, CuTMPP:

5,10,15,20-tetrakis(4-methoxycarbonylphenyl)porphyrin (TMPP, 1 g, 1.18 mmol) was dissolved in 150 mL of chloroform in a 500 mL round bottom flask. A solution of 10 eq. of copper acetate monohydrate (2.36 g) in a minimum amount of methanol was prepared separately and added to the former solution. Then, the reaction mixture was refluxed for 30 minutes. After cooling down to room temperature, the reaction crud was washed with distilled water to remove excess copper acetate. The organic layer was dried over anhydrous MgSO$_4$. The desired compound was eventually purified by column chromatography on silica gel using CHCl$_3$ as an eluent and then recrystallized in methanol/chloroform (10:1 v/v) and dried in a vacuum oven. Yield: 93% (0.99 g, 1.09 mmol). **UV-Vis (nm) in DCM:** 417, 539. **HRMS (ESI$^+$)**: calculated for [M+H$^+$]$^+$ 908.1902, found 908.1867 and calculated for [M+Na$^+$]$^+$ 930.1602, found 930.1696.

Synthesis of Copper(II)-2,3,7,8,12,13,17,18-octachloro-5,10,15,20-tetrakis (4-methoxycarbonylphenyl)porphyrinato, CuTMPPCl$_8$:

CuTMPP (500 mg, 0.55 mmol) was dissolved in 150 mL of chloroform and 12.5 eq. of NCS (900 mg) were added and the solution refluxed at 140 ^{0}C for 72 h. After the completion of the reaction, a saturated aqueous solution of sodium thiosulfate was added to this mixture to quench the reaction. The organic layer was then extracted, dried over anhydrous $MgSO_4$, and rotary-evaporated to give a solid. The crude product was purified by column chromatography on silica gel using DCM as eluent to give CuTMPPCl$_8$ in a 64% Yield (410 mg, 0.35 mmol). **UV-Vis (nm) in DCM**: 353, 437, 570.

Synthesis of 2,3,7,8,12,13,17,18-octachloro-5,10,15,20-tetrakis (4-methoxycarbonyl phenyl)porphyrin, TMPPCl$_8$:

CuTMPPCl$_8$ (400 mg, 0.34 mmol) was dissolved in 50 mL of chloroform, and 8 mL of concentrated H_2SO_4 were added dropwise at 0^{0}C, and the reaction mixture was stirred for 30 minutes. The organic layer was then extracted and washed with a saturated sodium bicarbonate aqueous solution and dried over anhydrous $MgSO_4$. The solvent was evaporated using a rotatory evaporator and the crude product was purified by column chromatography on silica gel using DCM/Acetone (99:1 v/v) as an eluent and recrystallized in DCM/Methanol (1:10 v/v) to give TMPPCl$_8$ in a 97% yield (390 mg, 0.35 mmol). **UV-Vis (nm) in DCM**: 358, 453, 550, 600, 710. **^{1}H NMR (300 MHz, CDCl$_3$) δ/ppm:** 8.46 (d, 8H, *meso-m*-phenyl-H), 8.28 (d, 8H, *meso-o*-phenyl-H), 4.12 (s, 12H, *meso-p*-CO2MePh-H).

Synthesis of 2,3,7,8,12,13,17,18-octachloro-5,10,15,20-tetrakis (4-methoxycarbonyl phenyl)porphyrin, TCPPCl$_8$:

TMPPCl$_8$ (250 mg, 0.22 mmol) was dissolved in 60 mL THF/MeOH (1:1 v/v), and a 30 mL 2M KOH solution was added. The reaction mixture was then refluxed for 48 hours. After that, it was cooled down to room temperature, and organic solvents were evaporated. The resulting aqueous solution was then acidified with 1M HCl solution until the total precipitation of the desired compound. Yield 89% (210 mg, 0.19 mmol). **UV-Vis (nm) in DMF**: 366, 467, 645. **^{1}H NMR (300 MHz, CDCl$_3$) δ/ppm** : 13.24 (s, 4H, *meso-p*-CO2HPh-H), 8.46 (d, 8H, *meso-m*-phenyl-H), 8.02 (d, 8H, *meso-o*-phenyl-H). **HRMS (ESI$^-$)**: calculated for $[M\text{-}H^+]^-$ 1060.8946, found 1060.8873 and Calculated for [M+2O (peroxyacid formation during the ionization)+OH$^-$]$^-$ 1114.9028, found 1114.8720.

References:

1. G. Paille et al. *J. Am. Chem. Soc*. **2018**, *140*, 3613-3618.

2. a) R. A. Marcus, *J. Chem. Phys*., **1956**, *24*, 966–978; b) R. A. Marcus, *J. Phys. Chem*., **1963**, *67*, 853–857; c) R. A. Marcus, *Angew. Chem., Int. Ed*., **1993**, *32*, 1111–1121.

3. A. Solé-Daura et al. *ACS Catal.* **2022**, *12*, 9244–9255.

4. R. Kumar, N. Chaudhary, M. Sankar and M. R. Maurya, *Dalton Trans.*, **2015**, *44*, 17720–17729.

5. G. A. Spyroulias, A. P. Despotopoulos, C. P. Raptopoulou, A. Terzis, D. de Montauzon, R. Poilblanc, and A. G. Coutsolelos, *Inorg. Chem.* **2002**, *41*, 2648–2659.

6. S. Zakavi, H. Yavari, A. Heydari-turkmani and L. Alghooneh, *J. Catal.*, **2020**, *387*, 84-94.